

Supplementary Materials

Effect of Nb and Ta Substitution on Donor Electron Transport and Ultrafast Carrier Dynamics in Anatase TiO₂ Thin Films

Kalon Gopinadhan^{1,4,*}, Brijesh Kumar¹, Natalie PALINA⁵, M. Motapathula¹, I. Pallecchi⁶, Y. Shihua¹, J. Q. Chen¹, T. P. Sarkar^{1,2}, A. Annadi^{1,2}, A. Rana¹, Amar Srivastava^{1,2}, D. Marré⁶, Jingsheng CHEN^{1,4}, Ariando^{1,2}, S. Dhar^{1,7}, A. Rusydi^{1,2,5} and T. Venkatesan^{1,3,4,*}

¹NUSNNI-NanoCore, National University of Singapore, Singapore 117576

²Department of Physics, National University of Singapore, Singapore 117542

³Department of Electrical and Computer Engineering, National University of Singapore, Singapore 117576

⁴Department of Materials Science and Engineering, National University of Singapore, Singapore 117575

⁵Singapore Synchrotron Light Source, National University of Singapore, Singapore 117603,

⁶CNR-SPIN and Università di Genova, Dipartimento di Fisica via Dodecaneso 33, Genova Italy 16146

⁷Department of Physics, Shiv Nadar University UP, India 201314

Further characterization of Nb and Ta substituted anatase TiO₂ epitaxial thin films

1. X-ray diffraction data for Ta substituted TiO₂ anatase thin films

X-ray diffraction data shown in Fig. S1(a) suggests that the films are purely anatase TiO₂ with only (004) and (008) reflections. The substitution of Ti with a pentavalent ion of Ta results an expansion of the lattice which is shown in Fig. S1(b).

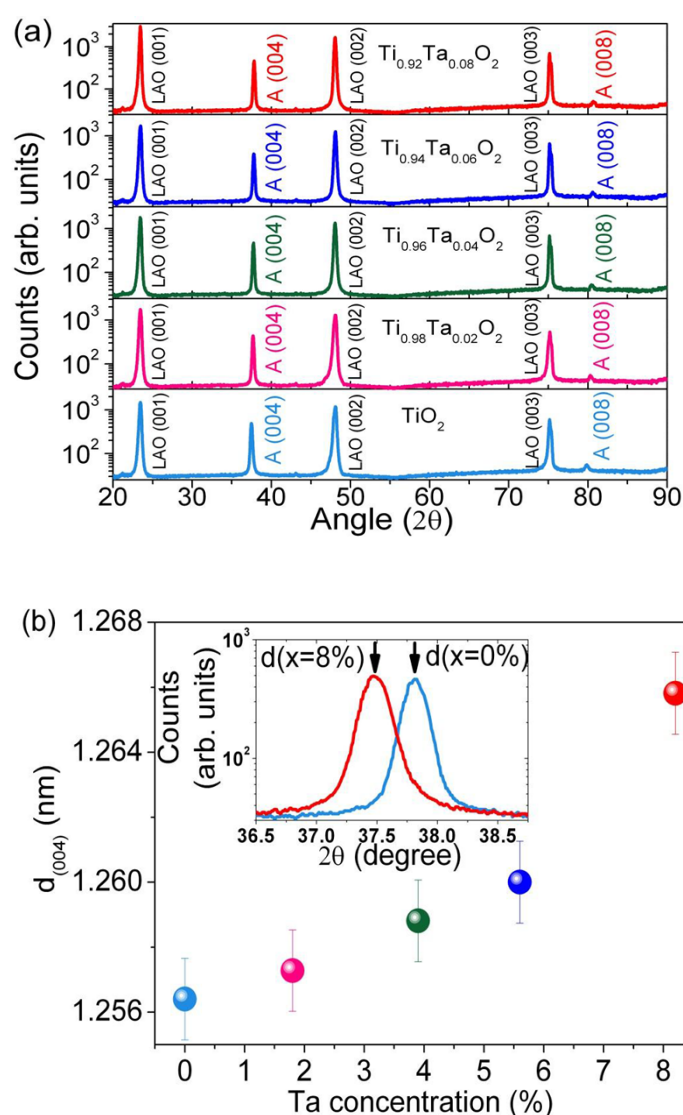


Figure S1:(a) X-ray diffraction θ - 2θ spectra for anatase Ti_{1-x}Ta_xO₂ ($x = 0 - 0.08$) thin films with the similar growth conditions described in the main text. (b) Variation of the d(004)

lattice parameter as a function of Ta concentration; (inset) shows the shift in the (004) anatase peaks for pure and 8% Ta incorporated TiO₂ films.

2. Temperature dependence of the carrier density

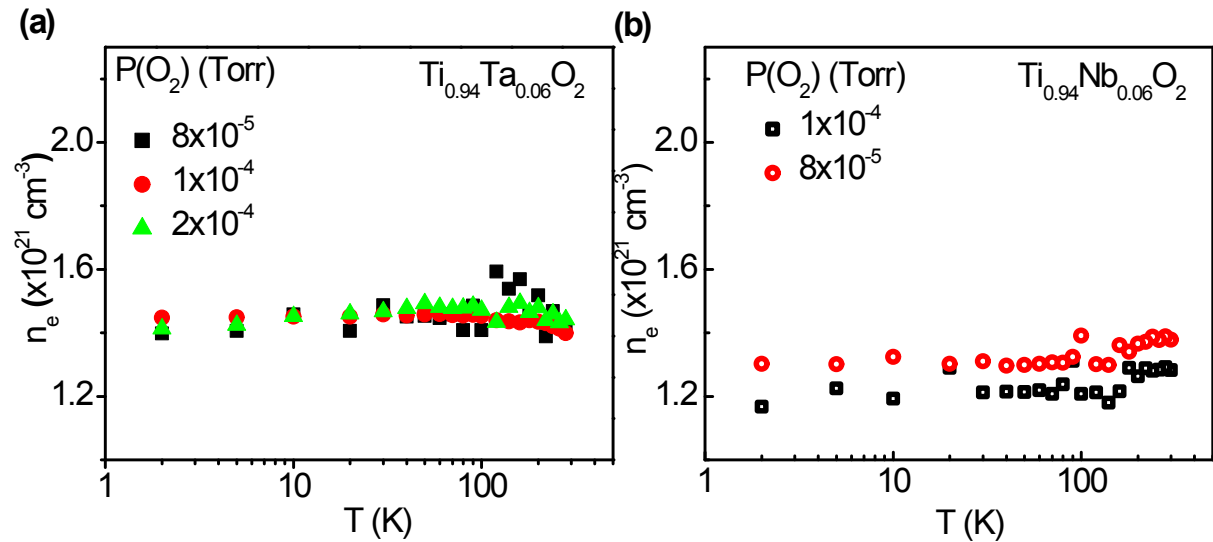


Figure S2: Carrier density of various films as a function of temperature for Ta and Nb substituted TiO₂ thin films. The carrier density is nearly temperature independent for both Ta and Nb substituted TiO₂ thin films suggesting the degeneracy of the donor electrons. The dependance of oxygen partial pressure on the carrier density is minimal in both Ta and Nb substituted TiO₂ thin films suggesting the minor role of oxygen vacancies.

3. Temperature dependent thermopower measurement to extract the effective mass of the carriers

Figure S3 shows the Seebeck coefficient S as a function of temperature for two representative samples from two different dopants. The comparison between resistivity and Seebeck curves versus temperature indicates that as long as the resistivity is metallic (positive temperature coefficient), the Seebeck coefficient is linear in T , as predicted by Mott law:

$$S = -\frac{\pi^2}{3e} K^2 T \frac{\partial \ln(\sigma(E))}{\partial E} \Big|_{E=E_F} \approx -\frac{\pi^2}{3e} K^2 T \left(\frac{\partial \ln(n)}{\partial E} \Big|_{E=E_F} + \frac{\partial \ln(\tau)}{\partial E} \Big|_{E=E_F} \right) \quad (1)$$

which yields for a degenerate semiconductor in 3D:

$$S = -\left(\frac{3}{2} + \alpha\right) \frac{8\pi^{8/3} K^2}{3^{5/3} h^2 e} m_{eff} \frac{T}{n_{3D}^{2/3}} \quad (2)$$

where α describes the functional dependence of the scattering time on the energy $\tau \sim E^\alpha$ and its value depends on the dominant scattering mechanism, K is the Boltzmann constant. For ionized impurity scattering, $\alpha \approx 1.5$, with acoustic phonons $\alpha \approx -0.5$ and for most other scattering mechanisms, α is between 0 and -1. For the fit, we initially assumed that α varies smoothly with temperatures, assuming $\alpha \approx 1.5$ at low temperature and -0.5 at high temperature. For the fit, the effective mass (m_{eff}), and carrier concentration (n_{3D}) are assumed to be constant, however the fit at low temperature is very poor in this case. The high temperature fit yields an electron effective mass of $2.1m_0$ for Ta:TiO₂ and $1.6m_0$ for Nb:TiO₂. The increase in effective mass relative to the free electron mass is a result of the interaction of electrons with phonons leading to large polaron formation. By considering a change in the nature of scattering mechanism at low temperature, we assume that the effective mass is a continuum which enables us to fit the thermopower data both for ionized impurity and acoustic phonon scattering.

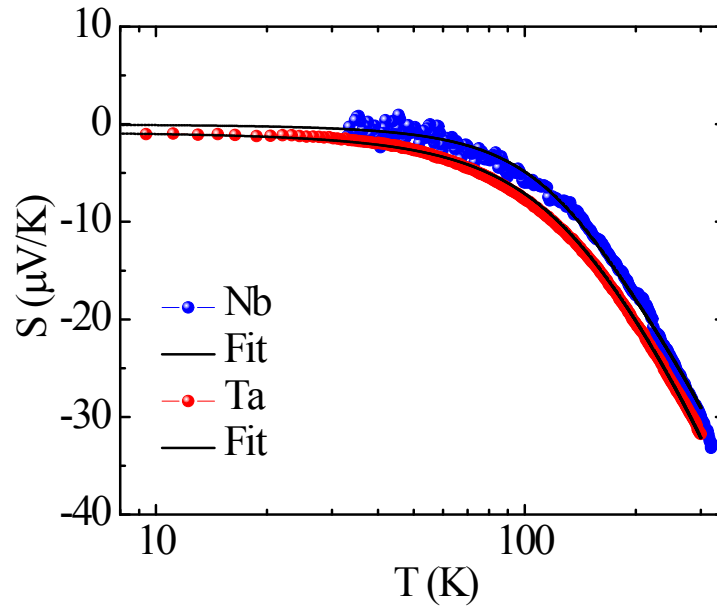


Figure S3: (a) Thermopower (S) as a function of temperature (T) for two representative samples one each from Nb and Ta substituted TiO_2 samples. The curves have been fitted by taking polaron contribution at high temperatures where the effective mass of the electrons are high due to interaction with phonons and an ionized impurity scattering at low temperatures where the effective mass is low.

4. Temperature dependence of the variation of the extracted carrier effective mass

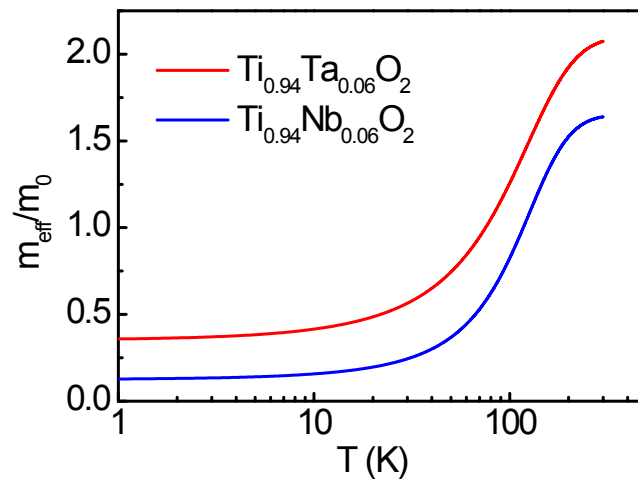


Figure S4: Variation of the effective mass of the conduction electrons as the temperature is lowered from 300 to 10 K. The variation in effective mass is due to a change in the nature of

the scattering. At high temperatures a stronger interaction between electron and phonon lead to an enhancement in the effective mass. However, as the temperature is lowered, the electron-phonon interaction is getting weaker, resulting a decrease in the effective mass.

5. Rutherford backscattering random and channelling spectra

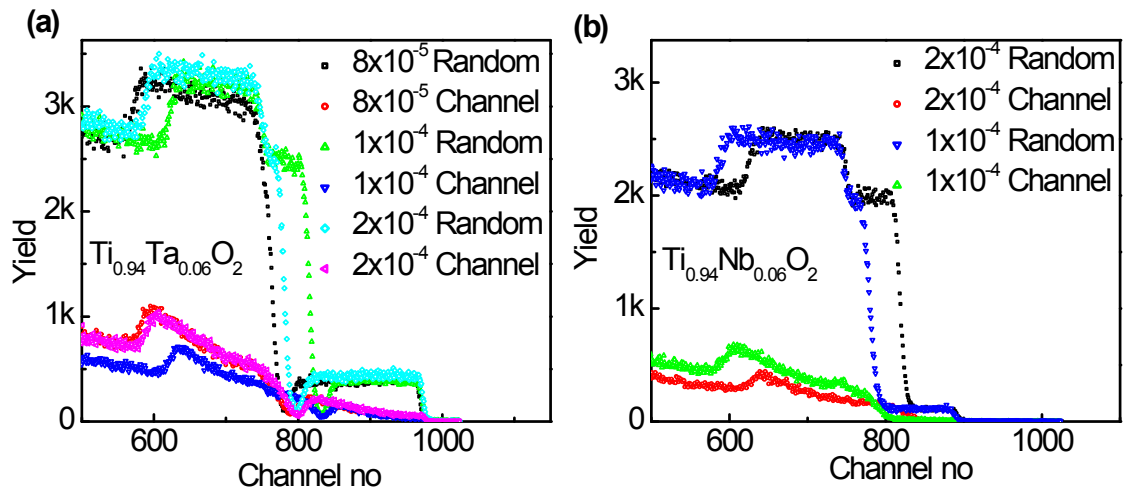


Figure S5: Rutherford backscattering (RBS) - random and channeling spectra collected for both Ta and Nb substituted TiO₂ thin films. In the case of Ta:TiO₂ sample prepared at PO₂=1x10⁻⁴ Torr, the minimum yield (χ) for Ti and Ta is 10 and 12% respectively and Ti substitutionality by Ta as 97.8%. In the case of Nb:TiO₂ sample prepared at PO₂=1x10⁻⁴ Torr, χ for Ti and Nb is 2.6 and 5.4% respectively, which yields the substitutionality of Ti by Nb as 97.1%. In addition, the percentage of Ti atoms occupying the lattice site is 97.4% suggesting that the percentage of off-site Ti atoms is only 2.6% which is much less when compared to Ta:TiO₂ sample. These results are in agreement with XPS and XAS data, further strengthening the conclusion that Ta:TiO₂ has more Ti vacancies (if all of the off-lattice atoms are attributed to be consist of vacancies) with less Ti³⁺ fraction whereas Nb:TiO₂ sample has more Ti³⁺ (corresponding to lattice site atoms) with less Ti vacancies.

6. Optical transmission in the normal incidence geometry

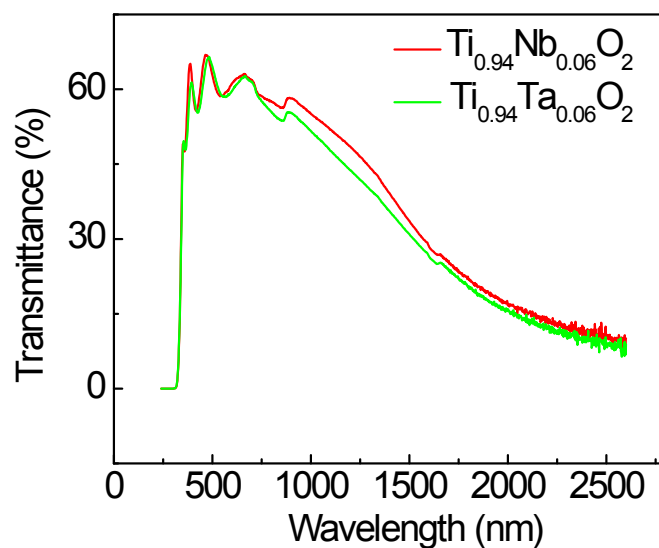


Figure S6: Transmittance of Ta and Nb substituted TiO_2 thin films ($P_{\text{O}_2} = 1 \times 10^{-4}$ Torr), indicating that the absorption starts below 360 nm and the band gap to be ~ 3.44 eV. Thickness fringes with maxima and minima are seen in the spectrum. The reduction of transmittance in the long wavelength is due to free carrier absorption resulting into the well known Drude conductivity tail.

7. Femtosecond transient spectroscopy of undoped anatase TiO_2 sample

Femtosecond transient reflectivity of undoped TiO_2 thin films has been performed at different time delays with an excitation wavelength of 350 nm and energy density $80 \mu\text{J}/\text{cm}^2$ which is shown in Fig. S7. The absorption related to t_{2g} to e_g appears as a dip in the reflectivity corresponding to a wavelength of 620 nm. There is no signature of any small and large polaron formation in the undoped TiO_2 sample strongly suggesting that Ta and Nb incorporation into TiO_2 induces polarons in the system.

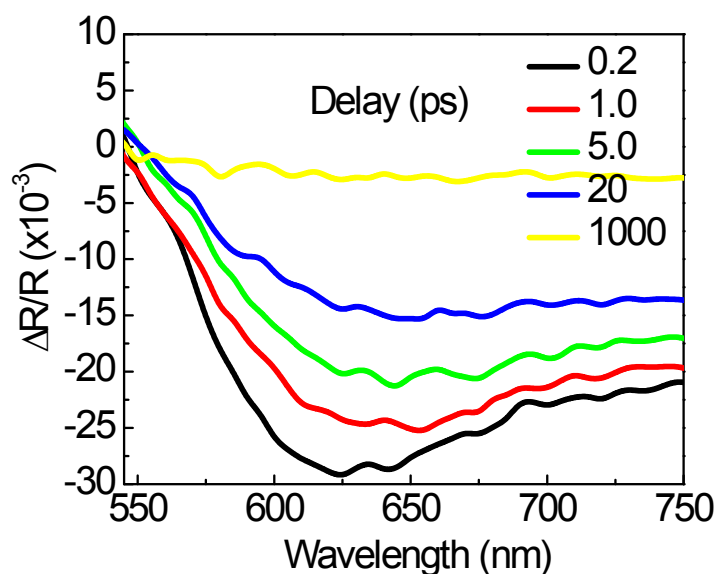


Figure S7: Femtosecond transient reflectivity of TiO₂ thin films at different time delays with an excitation wavelength of 350 nm and energy density of 80 μJ/cm².

8. Ellipsometric studies on Ta substituted TiO₂ samples

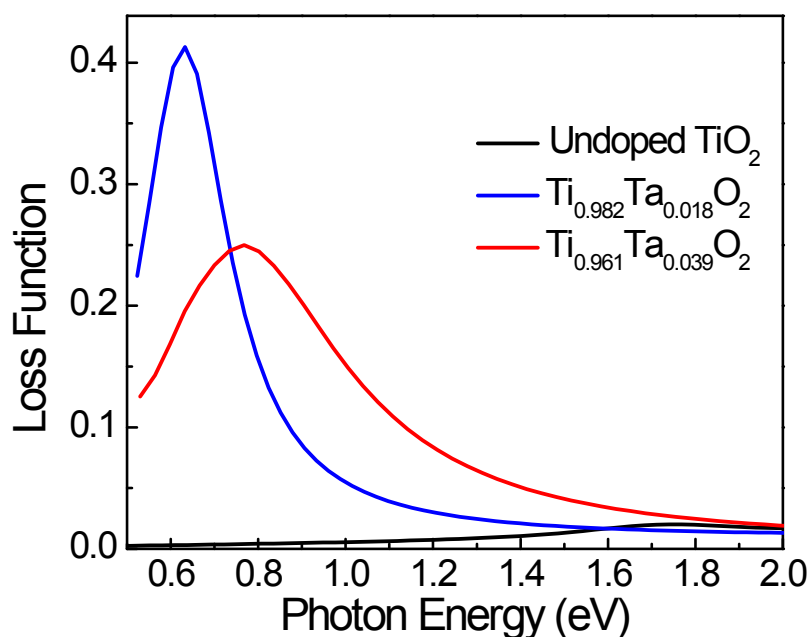


Figure S8: The Loss function extracted from Ellipsometric studies as a function of Ta substitution in TiO₂ samples. The small peaks found at 0.63 eV and 0.77 eV respectively for 1.8% and 3.9% Ta-substituted TiO₂ in the loss function spectrums could be due to small polaron formation. A blue-shift in polaronic peak is observed due to stronger electron-phonon

coupling with increasing Ta concentration. The decrease in intensity with increasing Ta might be attributed to an increase in the carrier density in the conduction band thus reducing the transition probability while the peak broadening might be due to increased lattice anharmonicity. Indeed, the recent angle resolved photoemission spectroscopy (ARPES) measurements on anatase TiO₂ with oxygen vacancies have shown a strong electron-phonon coupling and tunable polaronic conduction by carrier concentration^[1].

9. Explanation on why ionized impurity scattering is the most possible explanation for the low temperature resistance enhancement

Of several other possibilities for low temperature anomaly besides impurity scattering, the Altshuler-Aronov (AA) effect ^[2] predicts a logarithmic correction to the resistivity in disordered two dimensional electron systems due to electron-electron interactions, i.e. $\rho_{xx}(T) = \rho_{xx,0} + \delta\rho_{xx}(T)$, where $\delta\rho_{xx}(T) \sim \ln(T)$. In our case, since the film is very thick (~350 nm), the system is truly three dimensional with a mean free path much smaller than the thickness and therefore the possibility of AA effect is ruled out. The AA effect also predicts corrections to the Hall coefficient $R_H = R_{H,0} + \delta R_H(T)$, where $\delta R_H(T)$ is related to $\delta\rho_{xx}(T)$ by

$$\frac{\delta R_H(T)}{R_{H,0}} = 2 \frac{\delta\rho_{xx}(T)}{\rho_{xx,0}}$$

The electronic concentration doesn't vary with temperature and the temperature independent carrier density rules out AA effect in our sample. At very low temperatures, resistivity of our films is no more logarithmic in T but it varies as T^2 which rules out weak localization as the other possibility. The change in resistivity at low temperature is much larger than can be explained by weak localization. We also exclude Kondo effect as the possible cause of the resistivity upturn at low temperatures due to multiple reasons. The change in resistivity at low

temperature is much more than expected for a single magnetic impurity scattering. We observe a very weak negative magnetoresistance which is not in proportion to change in zero field resistivity at low temperatures. In addition, the negative magnetoresistance die out easily and a positive magnetoresistance appears beyond an applied magnetic field of 1 Tesla which is contrary to what expected for a single impurity Kondo effect with a reasonable Kondo temperature of 10 K.

REFERENCES

- [1] S. Moser, L. Moreschini, J. Jaćimović, O. S. Barišić, H. Berger, A. Magrez, Y. J. Chang, K. S. Kim, A. Bostwick, E. Rotenberg, L. Forró, M. Grioni, *Phys. Rev. Lett.* 2013, 110, 196403.
- [2] B. L. Altshuler, A. G. Aronov, P. A. Lee, *Phys. Rev. Lett.* 1980, 44, 1288.